Mon. Not. R. Astron. Soc. **310**, 360–376 (1999)

The ages of pre-main-sequence stars

Christopher A. Tout,[1,2]★ Mario Livio[2] and Ian A. Bonnell[1]
[1]*Institute of Astronomy, The Observatories, Madingley Road, Cambridge CB3 0HA*
[2]*Space Telescope Science Institute, 3700 San Martin Drive, Baltimore, MD 21218, USA*

Accepted 1999 July 2. Received 1999 June 18; in original form 1998 November 19

ABSTRACT

The position of pre-main-sequence or protostars in the Hertzsprung–Russell diagram is often used to determine their mass and age by comparison with pre-main-sequence evolution tracks. On the assumption that the stellar models are accurate, we demonstrate that, if the metallicity is known, the mass obtained is a good estimate. However, the age determination can be very misleading, because it is significantly (generally different by a factor of 2 to 5) dependent on the accretion rate and, for ages less than about 10^6 yr, the initial state of the star. We present a number of accreting protostellar tracks that can be used to determine age if the initial conditions can be determined and the underlying accretion rate has been constant in the past. Because of the balance established between the Kelvin–Helmholtz, contraction time-scale and the accretion time-scale, a pre-main-sequence star remembers its accretion history. Knowledge of the current accretion rate, together with an HR-diagram position, gives information about the rate of accretion in the past, but does not necessarily improve any age estimate. We do not claim that ages obtained by comparison with these particular accreting tracks are likely to be any more reliable than those from comparisons with non-accreting tracks. Instead, we stress the unreliability of any such comparisons, and use the disparities between various tracks to estimate the likely errors in age and mass estimates. We also show how a set of coeval accreting objects do not appear coeval when compared with non-accreting tracks. Instead, accreting pre-main-sequence stars of around a solar mass are likely to appear older than those of either smaller or larger mass.

Key words: accretion, accretion discs – stars: evolution – stars: formation – Hertzsprung–Russell (HR) diagram – stars: pre-main-sequence.

1 INTRODUCTION

The placement of an observed pre-main-sequence star in the theoretical Hertzsprung–Russell (HR) diagram ($\log L$ against $\log T_{\rm eff}$) is notoriously difficult because of its sensitivity to distance and reddening (see, e.g., Gullbring et al. 1998). In addition, any contribution to the light from the accretion disc itself must be subtracted, and obscuration by circumstellar material accounted for (see, e.g., Hillenbrand 1997). Here, by examining where theory predicts a particular object ought to lie at a given age, we investigate what properties of a pre-main-sequence star can be determined if these difficulties can be overcome.

The process by which stars form from their constituent interstellar material is as relevant to all branches of astrophysics, from planets to cosmology, as their subsequent evolution. However, our understanding and, without doubt, our predictive power lag well behind. This is partly because stars which are in the process of formation are more difficult to observe. The relative rapidity of the star formation process means that there are no nearby pre-main-sequence stars, and the fact that they form in denser regions of the interstellar medium favours observations at wavelengths longer than optical. It is only recently that such objects have begun to be observed in statistically significant numbers (Cohen & Kuhi 1979). From a theoretical point of view, difficulties arise because much of the process is dynamical and so does not lend itself well to the one-dimensional models normally employed in stellar evolution. On the other hand, we can model the hydrostatic inner regions using the methods normally employed in stellar evolution and so, with appropriate boundary conditions, approximate a forming star. Indeed, this kind of pre-main-sequence theory can be said to have begun alongside stellar evolution itself with the work of Henyey, Lelevier & Levee (1955), restricted to radiative solutions, and Hayashi (1961), with convection. These pioneers were able to describe how a spherical cloud of gas, already in hydrostatic equilibrium, contracts down to the main sequence as it releases its own gravitational energy.

The question of how the initial hydrostatic sphere forms is further complicated by two major effects. First, dynamical

★ E-mail: cat@ast.cam.ac.uk

© 1999 RAS

Downloaded from https://academic.oup.com/mnras/article/310/2/360/1047159 by guest on 16 May 2021

processes must be important in addition to thermal and nuclear and, second, these can no longer be expected to be spherically or even oblate-spheroidally symmetric. Larson (1969) modelled the spherically symmetric collapse of a gas cloud that is not yet in hydrostatic equilibrium. He showed how the central regions collapse first to form a hydrostatic core on to which the rest of the cloud accretes. However, this core cannot behave like Hayashi's pre-main-sequence stars, because its surface is no longer exposed to space and the boundary conditions are different. Larson introduced shock conditions at the surface of a near hydrostatic core. Building heavily on this, Stahler, Shu & Taam (1980a,b, 1981) were able to follow the evolution of the accreting core. Such a core, shrouded in its own accreting envelope, remains invisible as long as it accretes. Stahler et al. assumed that accretion and obscuration cease at the same time when the surrounding material is somehow blown away. Their stars then descend the classic Hayashi tracks until they develop radiative envelopes and move on to the corresponding Henyey track. However, if the accreting material does not obscure the entire stellar surface, we are able to see the star whilst it is still accreting. It is this latter situation that we model in this work. It is likely to arise because material accreting from far off will have too much angular momentum to fall radially on to the central core. Instead, it will form an accretion disc in a plane perpendicular to the angular momentum axis, and fall on to the core only as viscosity allows a small amount of material to carry the angular momentum outwards. If the disc reaches to the stellar surface, then the material will accrete only in an equatorial band. If, on the other hand, the central core possesses a magnetic field strong enough to disrupt the inner parts of the disc, matter might finally flow in along field lines accreting at relatively small magnetic poles or thin accretion curtains. Similar processes are known to operate in magnetic cataclysmic variables (see Warner 1995 for a review). In any of these cases, most of the stellar surface is left exposed and free to radiate like a normal star.

A comprehensive study of such exposed protostellar cores was made by Mercer-Smith, Cameron & Epstein (1984). Because more than the usual insight is needed to elucidate what they actually did, this work has largely been forgotten. However, it turns out that their accreting tracks qualitatively differ from ours,

Downloaded from https://academic.oup.com/mnras/article/310/2/360/1047159 by guest on 16 May 2021

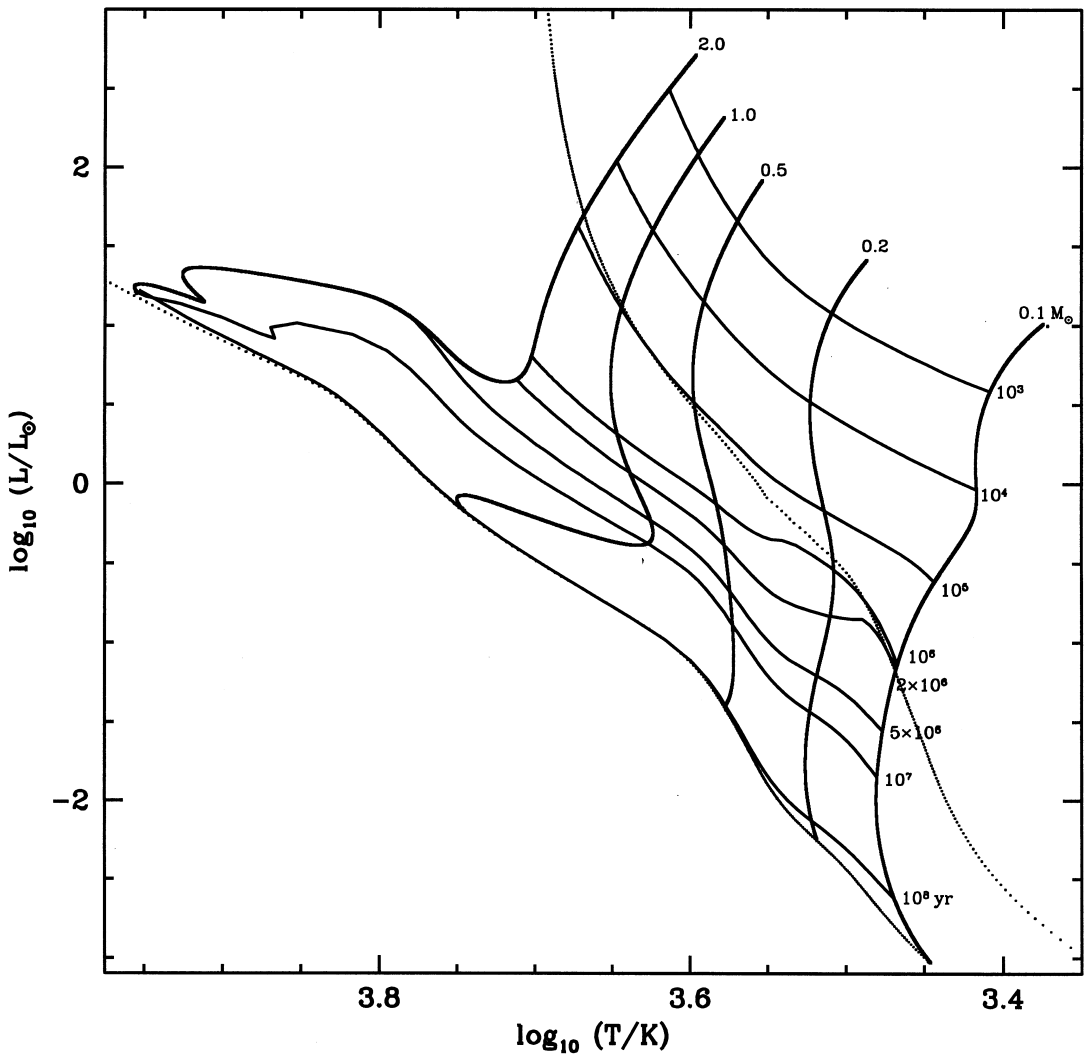

Figure 1. A Hertzsprung–Russell diagram showing constant-mass pre-main-sequence tracks of solar metallicity ($Z = 0.02$) stars in the range 0.1 to 2.0 $M_\odot$. Isochrones of ages ranging from 10^3 to 10^8 yr are drawn across the tracks. The models were begun at radii large enough that these isochrones are not affected by small displacements of this starting point. The zero-age main and deuterium-burning sequences appear as dots logarithmically spaced in mass.

and so it is important to identify exactly why this is. Their calculations begin with a hydrostatic core of $0.0015\,M_\odot$ of apparently $2\,R_\odot$ based on the dynamical collapse calculations of Winkler & Newman (1980). We shall argue in Section 3 that, at this mass, the core is still embedded in a rapidly collapsing cloud, and that something like $0.1\,M_\odot$ and $3\,R_\odot$ gives a more realistic representation of the central core when non-spherical accretion begins in earnest. However, we shall also show that the subsequent evolution is not overly sensitive to this initial state. More significantly, Mercer-Smith et al. require that at least one-quarter of the accretion luminosity be radiated uniformly over the whole stellar surface, while we claim that it can all be radiated locally in a disc boundary layer or localized shocks. This, coupled with their extreme accretion rates of typically $10^{-5}\,M_\odot\,yr^{-1}$, most probably accounts for the huge discrepancy between their and our tracks, manifested by the fact that their standard model is at a much higher effective temperature for a given mass than ours. As a consequence, our models evolve smoothly even if the accretion rate is abruptly changed, while theirs relax to a normal Hayashi track rapidly over about 100 yr when accretion is halted.

A careful analysis of the effects of accretion on stellar structure has been made by Siess & Forestini (1996), who vary a number of the physical properties of the accreted material relative to the stellar surface from angular momentum content to internal energy, and find that reasonable values of these parameters have little affect on the stellar structure. Siess, Forestini & Bertout (1997) then went on to use their formalism to follow a small number of evolutionary sequences. They confirmed the lack of sensitivity to their various parameters, except for the dependence on the fraction, α, of the accretion boundary-layer energy released below the stellar photosphere. Large values of this parameter are similar to Mercer-Smith et al.'s formalism, while our models correspond to $\alpha = 0$. Siess et al.'s models with $\alpha = 0.01$ are indeed very similar to our tracks when the accretion history is comparable.

We present several evolution tracks for pre-main-sequence stars accreting from various initial conditions, to quantify the accuracy to which age can be determined. Most of the tracks are for a solar

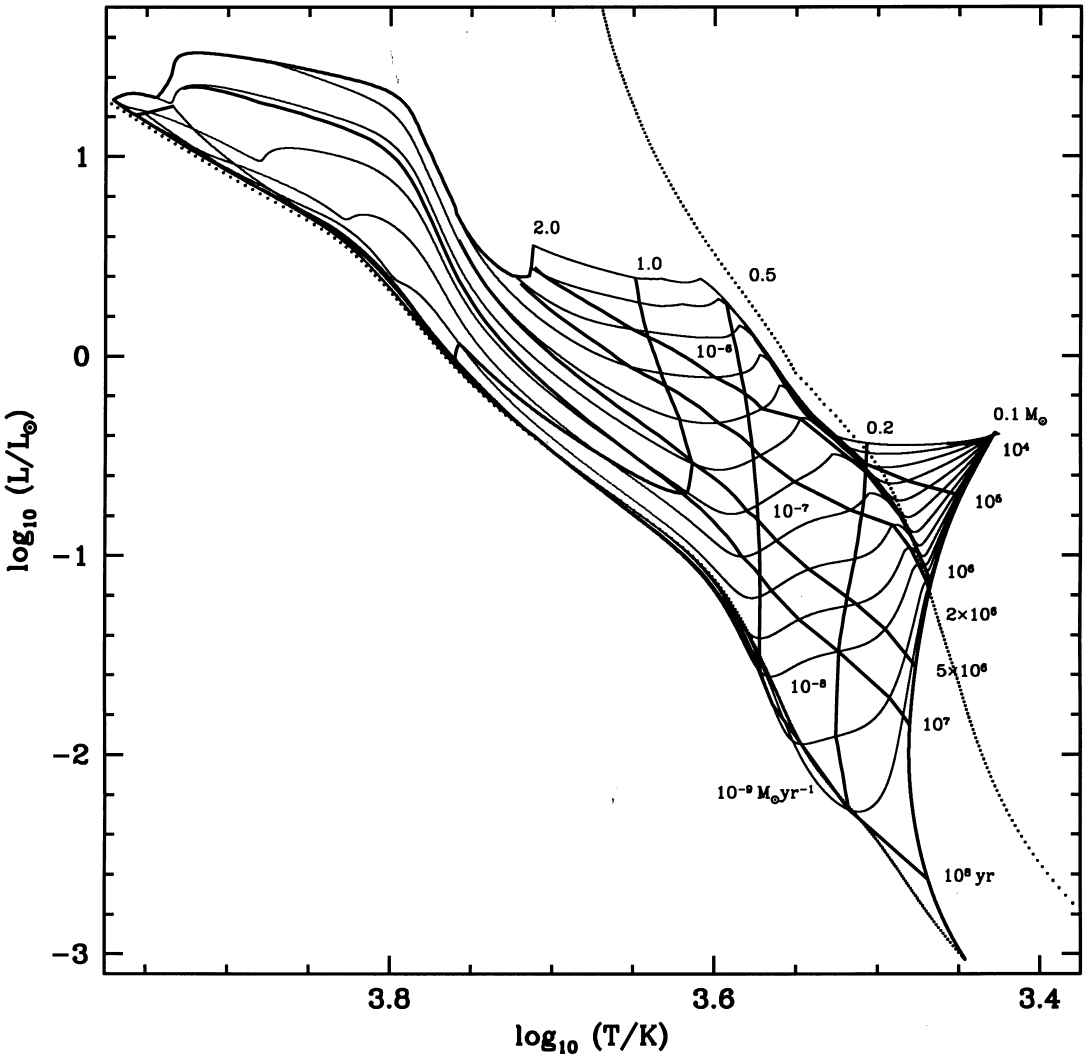

Figure 2. A Hertzsprung–Russell diagram showing, as thin lines, tracks followed by pre-main-sequence stars of initial mass $0.1\,M_\odot$ and radius $3\,R_\odot$ evolved with constant accretion rates ranging from 10^{-9} to 10^{-8} in steps of $10^{0.5}$ and then to $10^{-5.5}\,M_\odot\,yr^{-1}$ in steps of $10^{0.25}$ to a final mass of $2\,M_\odot$. Thick lines are isochrones of 10^4 to 10^8 yr or join points of equal mass from 0.1 to $2.0\,M_\odot$. The zero-age main and deuterium-burning sequences appear as dots logarithmically spaced in mass.

Downloaded from https://academic.oup.com/mnras/article/310/2/360/1047159 by guest on 16 May 2021

metallicity of $Z = 0.02$. However, measurements of metallicity in Orion's star-forming regions, though highly uncertain, indicate that $Z = 0.001$ may be more appropriate (Rubin et al. 1997). Such low metallicity is also typical of star-forming regions in the Large Magellanic Cloud. We therefore discuss a set of low-metallicity tracks which demonstrate how both mass and age determinations from colour–magnitude diagrams depend critically on a knowledge of metallicity. Because the stellar mass function dictates that the bulk of stars have final masses on the low side, we restrict our presentation here to accreting objects of less than $2\,M_{\odot}$. We can expect almost all stars in the star-forming regions with which we may wish to compare properties to lie below this mass. Also, as stressed by Palla & Stahler (1993), the contraction time-scales for massive stars are short compared with accretion time-scales, so that the accreting tracks will tend to follow the zero-age main-sequence (ZAMS), and the effective pre-main-sequence life of massive stars is dominated by their early, low-mass evolution. Indeed, at higher masses the accretion time-scale becomes long compared with the nuclear time-scale, and it is difficult to separate pre- and post-main-sequence evolution for some stars.

We find that masses can be fairly well established if the metallicity is known, but that ages are very dependent on the accretion history and the initial state of the star, particularly below 5×10^6 yr. However, before we can begin to discuss age determination, we must first establish to what this age is relative.

2 THE ZERO AGE

It is very often unclear how to define the zero-age point for a forming star, and of course it is rather uninformative to quote an age t without explaining exactly what we mean by $t = 0$. For evolved stars the ZAMS provides a convenient starting point from which we can both begin the evolution and measure the age of the star. The ZAMS must then be defined. Historically, a star was started in a state of hydrostatic and thermal equilibrium with a uniform initial composition. In reality, a star never actually passes through this zero-age state, because some nuclear burning takes place while a newly formed star is still contracting to the main sequence. In practice, because the thermal-evolution time-scale of pre-main-sequence stars is several orders of magnitude shorter than the post-main-sequence nuclear time-scale, very little of the

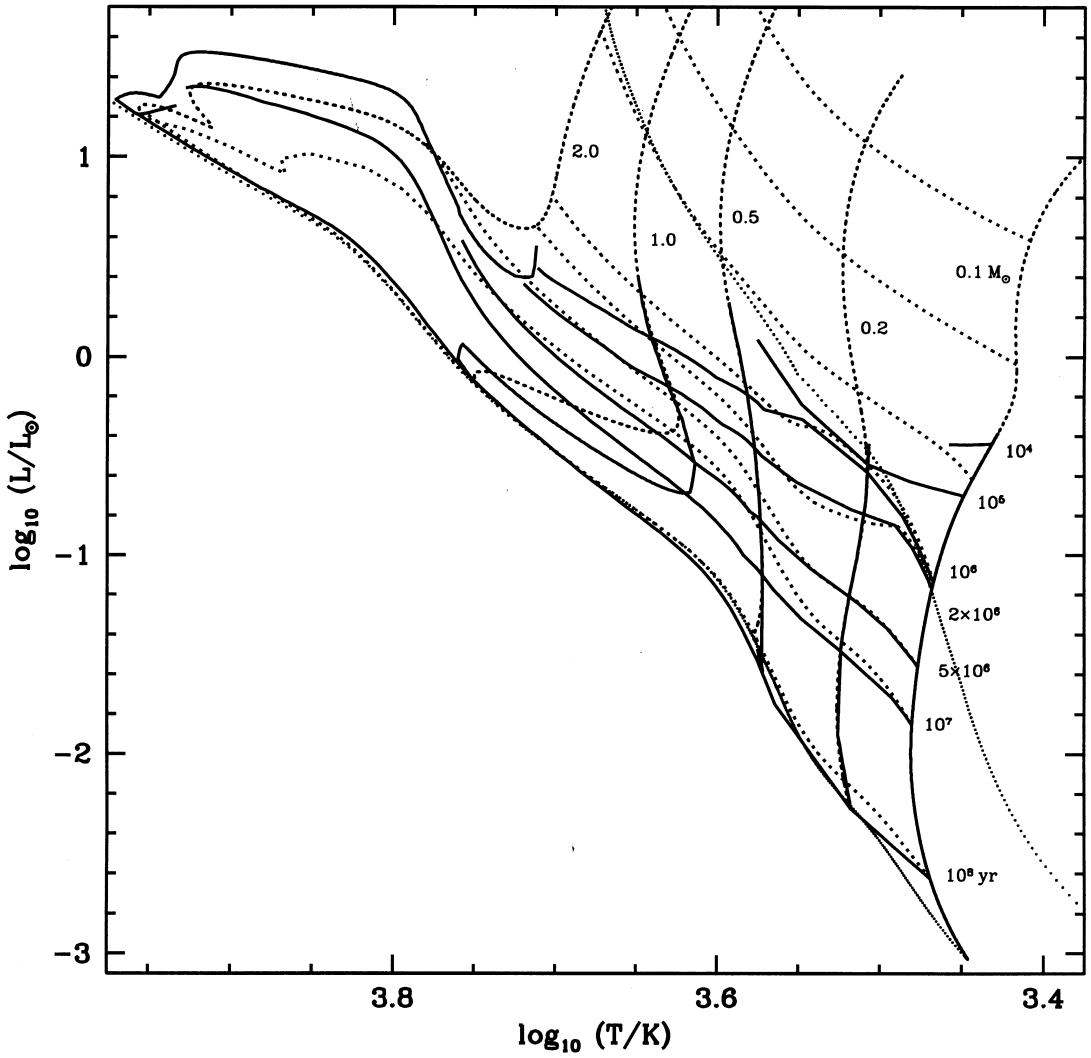

Figure 3. The isochrones and equal-mass loci from Fig. 2 – solid lines – overlaid with the pre-main-sequence tracks and isochrones of Fig. 1 – dotted lines. The zero-age main and deuterium-burning sequences appear as dots logarithmically spaced in mass.

Downloaded from https://academic.oup.com/mnras/article/310/2/360/1047159 by guest on 16 May 2021

initial hydrogen is burnt, and a uniform hydrogen abundance throughout the star is a reasonable approximation. This is not so for the catalytic elements of the CNO cycle in sufficiently massive stars, because these elements are driven towards equilibrium during pre-main-sequence evolution. Even so, it is possible to define a ZAMS (see, e.g., Tout et al. 1996) that roughly corresponds to the minimum luminosity attained as a star evolves from a pre- to post-main-sequence phase. Nor is the assumption of uniform abundance true for the elements involved in the pp chain, notably deuterium and He^3. However, on the ZAMS, the pp chain is complete in transforming hydrogen to He^4 at the stellar centres, and so the abundances of deuterium and He^3 are in equilibrium for given temperatures and number densities, and subsequently need not be followed explicitly. On the other hand, deuterium burning is a major source of energy in pre-main-sequence stars, and is important throughout this work.

Because we can define a ZAMS reasonably uniquely, a good way to measure pre-main-sequence ages would be backwards from the ZAMS. However, this is not acceptable if one wishes to measure the time elapsed since the birth of a star, where relatively small changes in age lead to large excursions in the HR diagram. A similar problem is encountered with the upper parts of the red giant, and particularly asymptotic giant, branch, but in these cases we regard absolute age as relatively useless, preferring such quantities as degenerate core mass as a measure of the evolutionary state (Tout et al. 1997).

The concept of a stellar birthline in the HR diagram was introduced by Stahler (1983) as the locus of points at which stars forming from a spherically accreting cloud would first become visible. In the model of Stahler, Shu & Taam (1980a,b, 1981) this occurs when deuterium ignites in the protostellar core and some ensuing wind blows away the remainder of the accreting cloud which has, up to this point, shrouded the star itself from view. With such a theory, a perfect place to fix the zero age of a pre-main-sequence star would be the onset of deuterium burning. Deuterium burning provides pressure support for the star for a time comparable with the Kelvin–Helmholtz time-scale τ_{KH}, on which it contracts once deuterium is exhausted. This time-scale is similar to the entire time taken to contract to this point from any initial state, so that by the time a star begins to contract again, below the deuterium-burning sequence, it is already relatively old and has a reasonably well-defined age. Here we concern ourselves

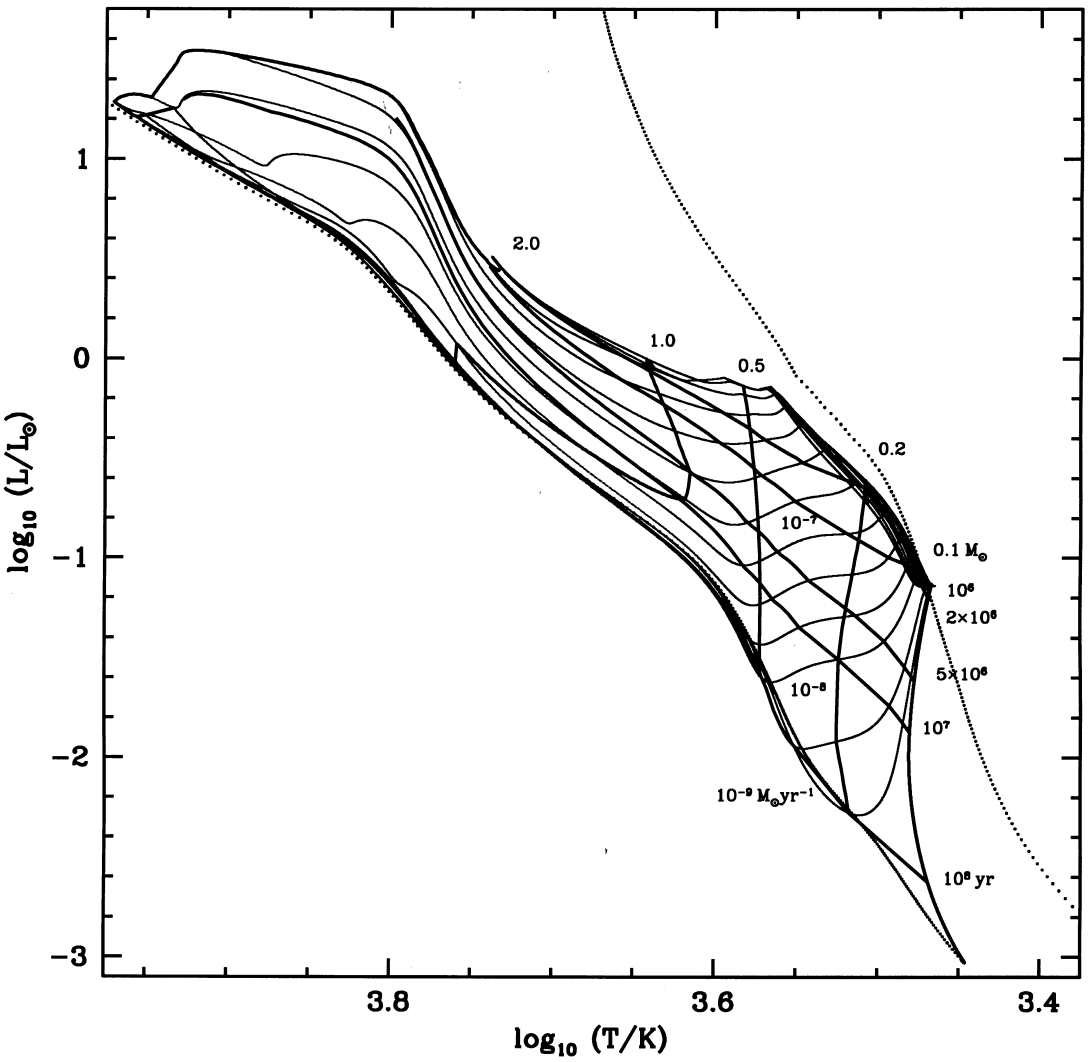

Figure 4. As Fig. 2 but for pre-main-sequence stars of initial mass 0.1 $M_\odot$ and radius such that the initial model is just about to cross the deuterium-burning sequence.

Downloaded from https://academic.oup.com/mnras/article/310/2/360/1047159 by guest on 16 May 2021

with accretion through a disc. In this case most of the stellar photosphere is exposed while accretion is still taking place. Nor do we assume that accretion ceases at the onset of deuterium burning. Under such circumstances there is no reason why stars should not appear above Stahler's birthline, and it is no longer possible to define a birthline as a locus of maximum luminosity at which pre-main-sequence stars appear. However, the interruption of contraction when deuterium ignites means that we are much more likely to see stars on and below the deuterium-burning sequence than above it. By definition, Stahler's birthline is more or less coincident with the deuterium-burning sequence, and this explains the consistency of observations with the idea of a birthline. Unfortunately, this apparent birthline is not the place where stars are born, and so an age measured from a zero-age deuterium-burning sequence is too young by an unknown amount which is normally at least as much as the deuterium-burning lifetime.

D'Antona & Mazzitelli (1994) take another approach, which is to begin evolution at a point in the HR diagram of sufficiently high luminosity, or equivalently at sufficiently large radius on a Hayashi track, that $\tau_{\rm KH}$ is much less than some acceptable error in the age at any later time. This error might be chosen to be about 100 yr. Such a definition leads to a well-defined age at any point on a track corresponding to a constant mass. For comparison, Fig. 1 shows such a set of pre-main-sequence tracks for $M = 0.1$, 0.2, 0.5, 1 and $2\,{\rm M}_{\odot}$, and isochrones fitted to 50 models in this range. We describe our models in detail in the following sections, but note that, because we use very similar physics, they do not differ greatly from those of D'Antona & Mazzitelli.

However, stars do continue to accrete long after their photospheres are exposed, and they can be placed in an HR diagram. A star of about $1\,{\rm M}_{\odot}$ is most unlikely to have reached this mass while $\tau_{\rm KH}$ was still small, or indeed even before deuterium exhaustion. For this reason we take the zero-age point of each of our tracks to be a point at which the protostellar core has the mass and radius of a typical self-gravitating fragment of a protostellar cloud, and model the subsequent evolution with ongoing accretion. We then investigate how changing these initial conditions alters the subsequent isochrones in the HR diagram to get an idea of how well we can constrain the age of an observed pre-main-sequence star relative to its birth as a self-gravitating accreting body.

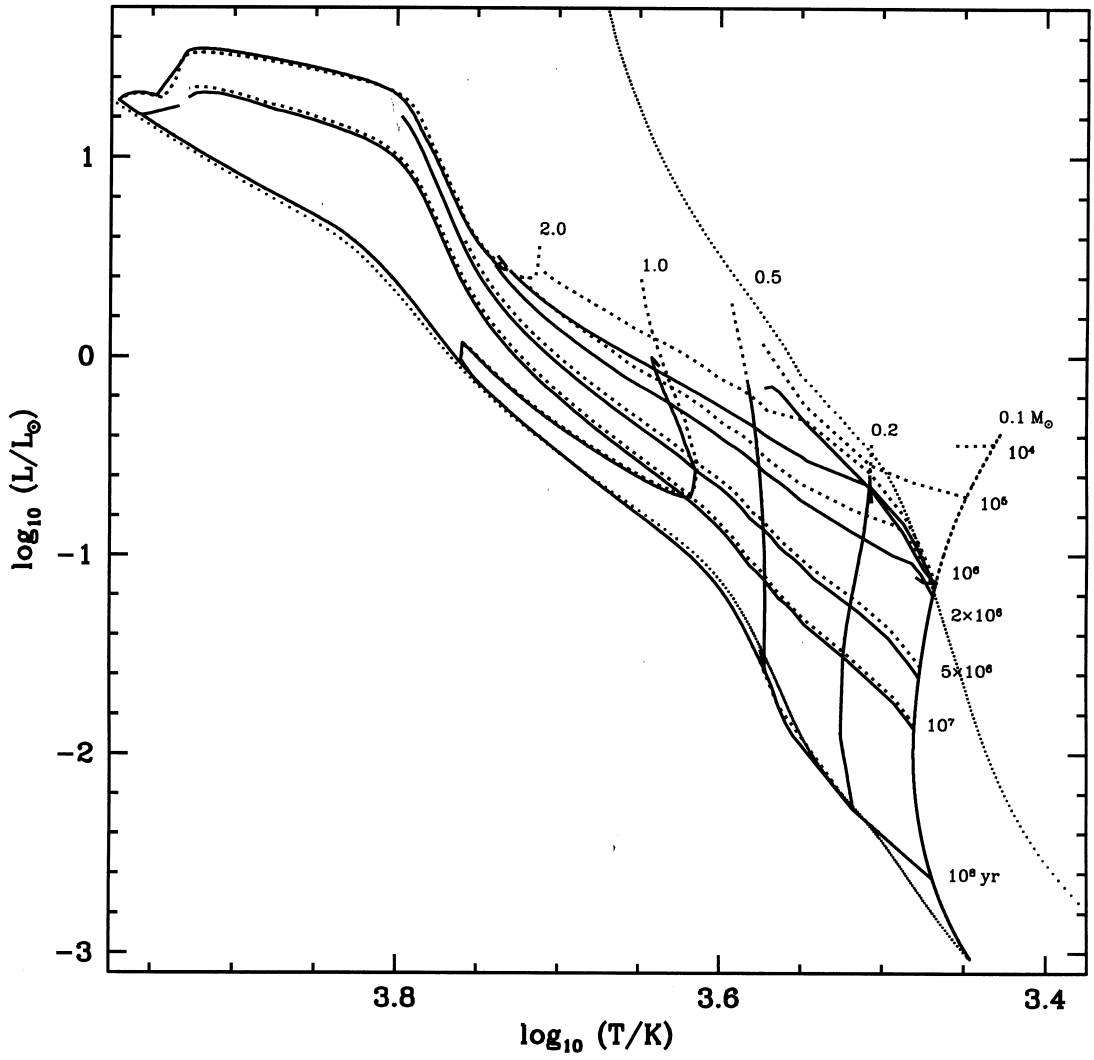

Figure 5. The isochrones and equal-mass loci of Fig. 4 – solid lines – overlaid with our standard ones from Fig. 2 – dotted lines.

Downloaded from https://academic.oup.com/mnras/article/310/2/360/1047159 by guest on 16 May 2021

3 THE STELLAR MODELS

We construct our stellar models using the most recent version of the Eggleton evolution program (Eggleton 1971, 1972, 1973). The equation of state, which includes molecular hydrogen, pressure ionization and Coulomb interactions, is discussed by Pols et al. (1995). The initial composition is taken to be uniform with a hydrogen abundance $X = 0.7$, helium abundance $Y = 0.28$, deuterium abundance $X_D = 3.5 \times 10^{-5}$ and metal abundance $Z = 0.02$ with the meteoritic mixture determined by Anders & Grevesse (1989). Hydrogen burning is allowed by the pp chain and the CNO cycles. Deuterium burning is explicitly included at temperatures too low for the pp chain. Once the pp chain is active, hydrogen is assumed to burn to He^4 via deuterium and He^3 in equilibrium. The burning of He^3 is not explicitly followed. Opacity tables are those calculated by Iglesias, Rogers & Wilson (1992) and Alexander & Ferguson (1994). An Eddington approximation (Woolley & Stibbs 1953) is used for the surface boundary conditions at an optical depth of $\tau = 2/3$. This means that low-temperature atmospheres, in which convection extends out as far as $\tau \approx 0.01$ (Baraffe et al. 1995), are not modelled perfectly. However, the effect of this approximation on observable quantities is not significant in this work (see, e.g., Kroupa & Tout 1997).

We assume that material is accreted from a disc on to a thin equatorial region of the star, so that normal photospheric boundary conditions are appropriate over most of its surface. This would also be true even if the inner edge of the disc is magnetically disrupted and the material funnelled to a few spots or narrow accretion curtains whose areas represent a relatively small fraction of the stellar surface. Because our models are one-dimensional, we must apply these same boundary conditions over the whole surface. Similarly, we must assume that accreted material is rapidly mixed over this same complete surface so that, on accretion of mass δM, we can add a spherical shell of mass δM with composition equal to the initial, or ambient, composition. We note that the photospheric boundary conditions effectively fix the thermodynamic state of the accreted material to those conditions over the radiating stellar surface. This is equivalent to the assumption that boundary layer shocks or, in the case of magnetically funnelled accretion, shocks at or just above the stellar surface remove any excess entropy from the accreting material, and so it is not unduly restrictive. Ideally, we would like to treat this problem in two dimensions. We could then apply

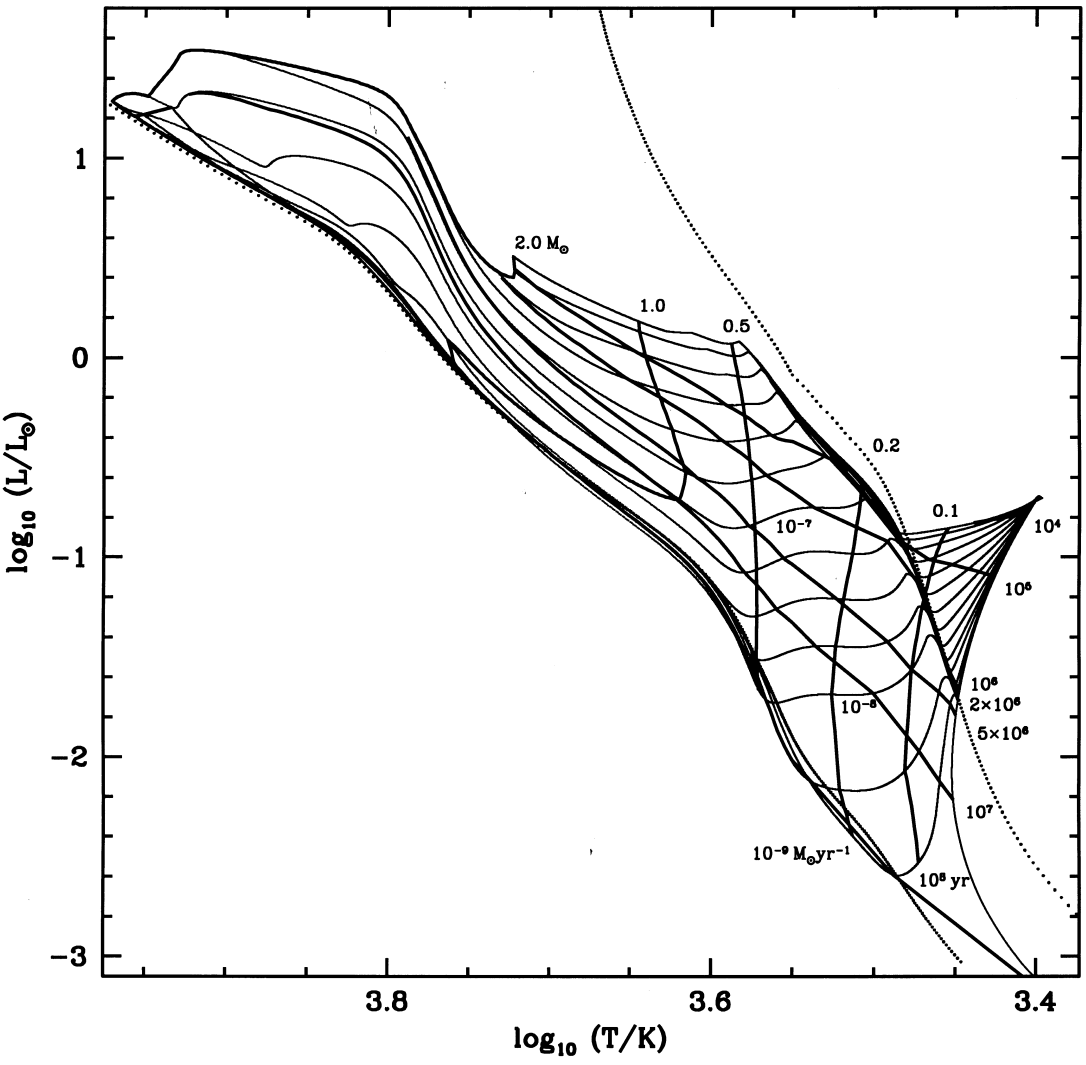

Figure 6. As Fig. 2 but for pre-main-sequence stars of initial mass $0.05\,M_\odot$ and radius $2.4\,R_\odot$.

Downloaded from https://academic.oup.com/mnras/article/310/2/360/1047159 by guest on 16 May 2021

different boundary conditions over the equatorial band or polar spots where accretion is actually taking place. With current computational power and techniques such models may not be too far off (Tout, Cannon & Pichon, private communication).

4 INITIAL CONDITIONS

We wish to take as an initial model a typical protostellar core of mass M_0 that is self-gravitating within a cloud and that has reached hydrostatic but not yet thermal equilibrium out to a radius R_0. Additional material beyond R_0 may be gravitationally bound to the star but not yet accreted. We assume that the core is spherically symmetric out to R_0, and that beyond this radius material sinks on to a disc from which it is accreted in a thin equatorial band or other relatively small part of the stellar photosphere.

The technique we use to construct the initial model is fairly standard. We take a uniform-composition ZAMS model of mass M_0 and add in an artificial energy generation rate ϵ_c per unit mass uniformly throughout the star. Initially, ϵ_c is negligible, but we gradually increase it so that the star is slowly driven back up its Hayashi track. In a sense, ϵ_c mimics the thermal luminosity that would be released if the star were contracting down the Hayashi track. These objects, however, are in thermal equilibrium. We continue to increase ϵ_c until the radius of the object is considerably more than R_0. At this point we may add or subtract mass freely, while maintaining hydrostatic and thermal equilibrium, and so vary M_0. In this way we can reach masses below the hydrogen-burning limit that would not have a ZAMS state of their own. We then switch off the artificial energy generation and allow the star to contract down its Hayashi track supported by the usual gravitational energy release. When $R = R_0$ we have our initial model.

We choose a protostellar core of $M_0 = 0.1\,M_\odot$ and $R_0 = 3\,R_\odot$ as our standard initial model. This choice of the initial mass and radius of the pre-main-sequence star is necessarily somewhat arbitrary, because it depends on the pre-collapse conditions and the dynamics of the collapse process. We choose a mass and radius taken to represent a young star at the end of the collapse and spherical infall phase of evolution at a time when it first becomes optically visible. This will include the initial protostellar core that forms from the collapse phase, plus any mass that is accreted on to this core before the infall becomes significantly

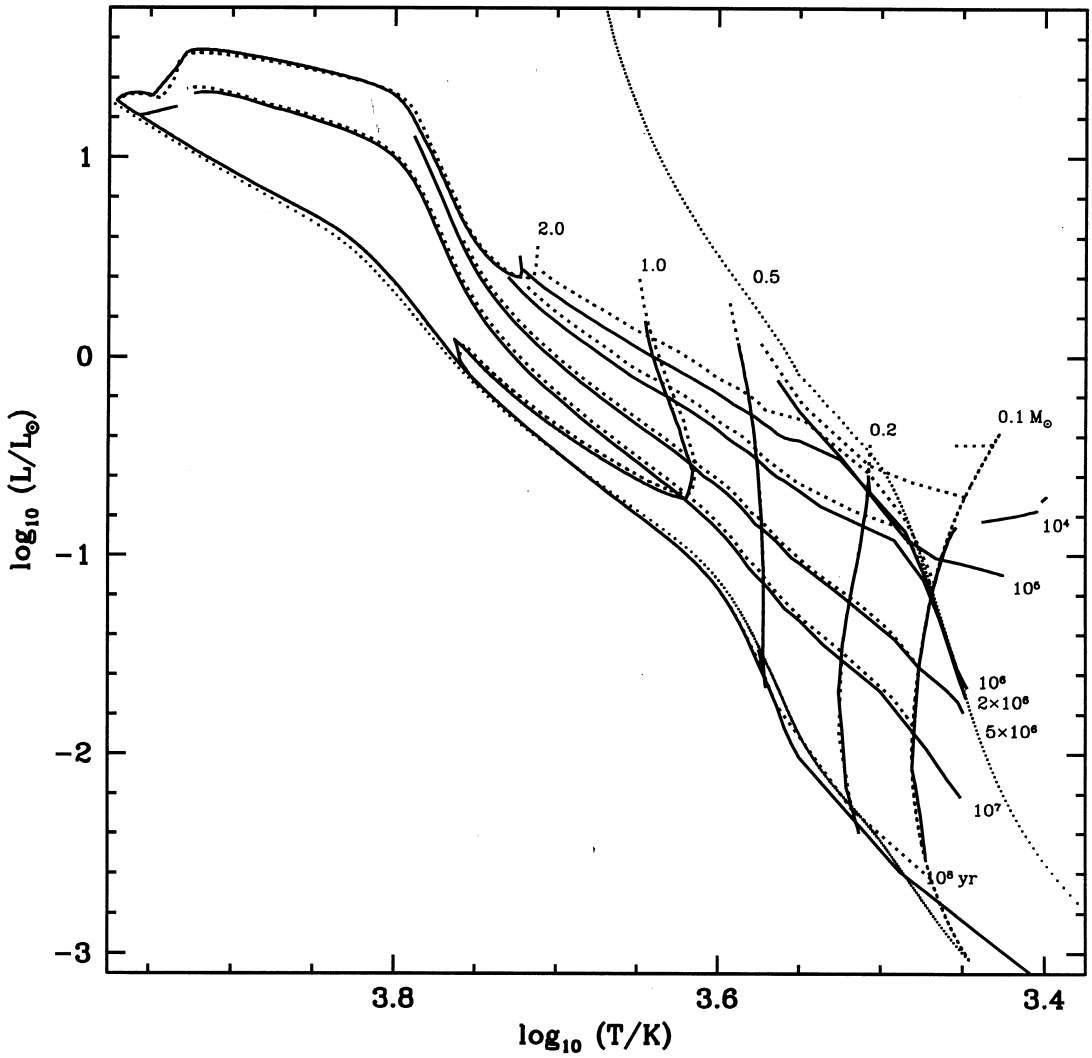

Figure 7. The isochrones and equal-mass loci of Fig. 6 – solid lines – overlaid with our standard ones from Fig. 2 – dotted lines.

Downloaded from https://academic.oup.com/mnras/article/310/2/360/1047159 by guest on 16 May 2021

aspherical. This happens when the infalling material has enough angular momentum to force it to collapse towards a disc rather than be accreted directly by the protostellar core. Any further accretion from this point will be through this circumstellar disc.

The gravitational collapse of a molecular cloud forms a first protostellar core when the density becomes large enough to trap the escaping infrared radiation (e.g. Larson 1969). This sets a minimum mass for opacity limited fragmentation at about $0.01\,M_\odot$ (Low & Lynden-Bell 1976; Rees 1976). This minimum mass will be increased by the material from further out with low angular momentum (along the rotation axis), plus the matter that has its angular momentum removed/redistributed by gravitational torques (e.g. Larson 1984) in the disc on time-scales short compared with the free-fall time. The accretion of low-angular-momentum matter probably increases the protostar's mass by a factor of 3 (for initially uniform density collapse). The accreted disc material can be estimated as that with dynamical times significantly less than the original free-fall time. Thus material within $20-50$ au should be accreted within 10^3 yr, which corresponds to disc sizes several times larger than the first core. For initially solid-body rotation and uniform cloud density this translates to a mass at least 3 times larger. We thus estimate our initial mass as about $0.1\,M_\odot$. This compares well to the mass of a protostellar core from a spherical collapse within a fraction of a free-fall time (Winkler & Newman 1980), and to the mass within 50 au in a collapse including rotation (Boss 1987; see also Lin & Pringle 1990). An initial mass of $0.1\,M_\odot$ is also comparable to the observed lower limit for stellar masses, and still allows for significant mass increase through subsequent accretion.

The choice of the initial stellar radius is perhaps more constrained. Estimates of this radius depend on the dynamics of the collapse, but are generally in the range of 2.5 to $3\,R_\odot$ (Winkler & Newman 1980; Stahler 1988). We have chosen the value of $3\,R_\odot$ as given by Winkler & Newman for an accreting protostar of

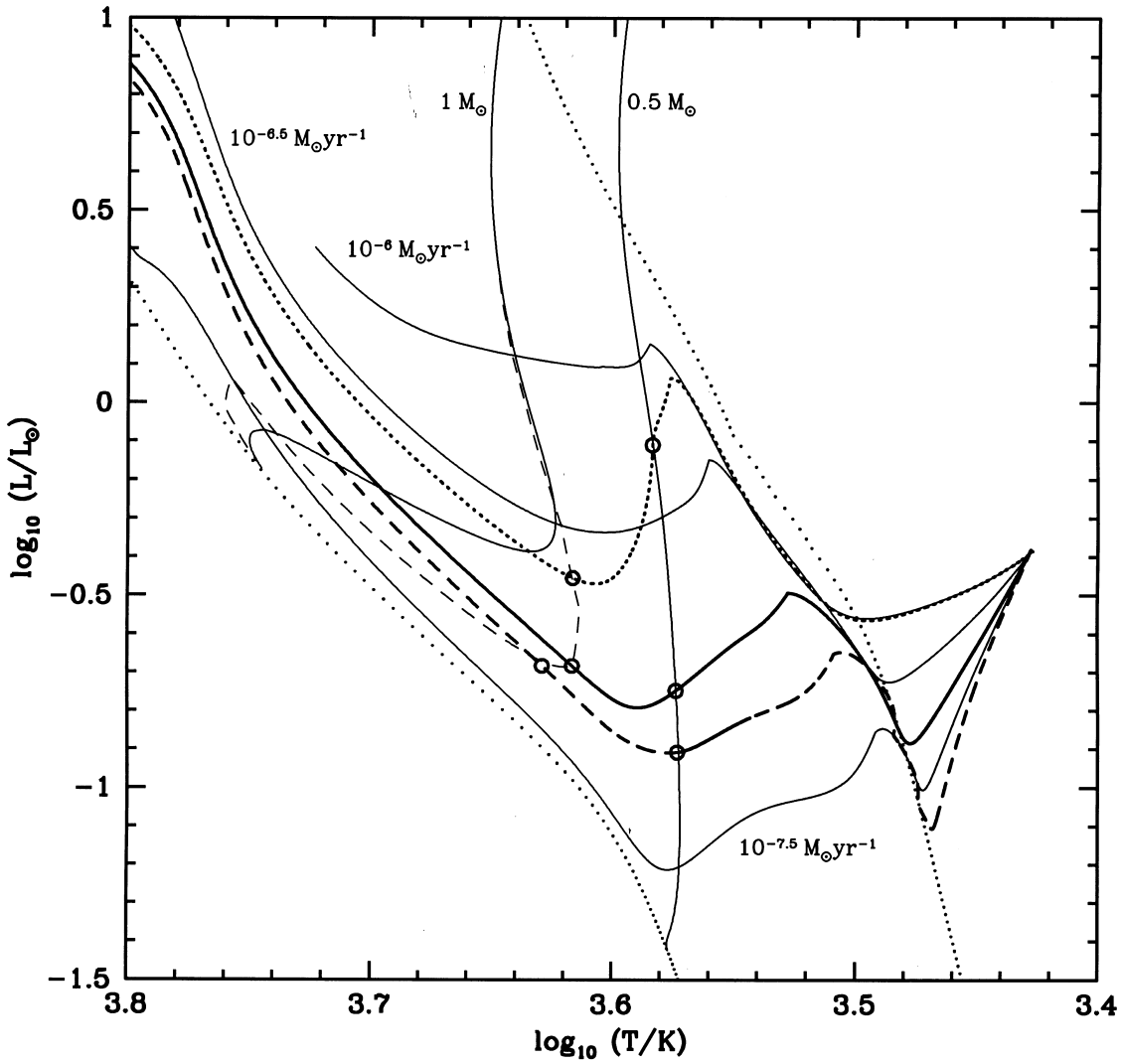

Figure 8. Three stars accreting at a constant rate of $10^{-7}\,M_\odot\,yr^{-1}$ from $0.5\,M_\odot$ upwards but reached by different routes from the same initial core of $M_0 = 0.1\,M_\odot$ and $R_0 = 3\,R_\odot$: solid line – constant $\dot{M} = 10^{-7}\,M_\odot\,yr^{-1}$; dashed line – linearly increasing from $\dot{M} = 0$ at $t = 0$ to $\dot{M} = 10^{-7}\,M_\odot\,yr^{-1}$ at $t = 8\times10^6$ yr when $M = 0.5\,M_\odot$; dotted line – linearly decreasing rate from $\dot{M} = 10^{-6}\,M_\odot\,yr^{-1}$ at $t = 0$ to $\dot{M} = 10^{-7}\,M_\odot\,yr^{-1}$ at $t = 7.3\times10^5$ yr when $M = 0.5\,M_\odot$. Open circles indicate masses of 0.5 and $1\,M_\odot$ for each of these tracks. Thin solid lines are our standard accreting tracks for $10^{-7.5}$, $10^{-6.5}$ and $10^{-6}\,M_\odot\,yr^{-1}$ and non-accreting tracks of 0.5 and $1\,M_\odot$, while the dashed line is the locus of $1\,M_\odot$ for the standard accreting tracks. Dots mark the zero-age sequences as elsewhere.

Downloaded from https://academic.oup.com/mnras/article/310/2/360/1047159 by guest on 16 May 2021

0.1 to greater than 0.5 $M_\odot$. We investigate variations in R_0 and M_0, and find that the precise choice is not very critical anyway.

5 STANDARD MODELS

From the standard initial conditions $M_0 = 0.1\,M_\odot$ and $R_0 = 3\,R_\odot$ we evolve a set of 13 pre-main-sequence stars accreting at constant rates of $10^{-5.5}$, $10^{-5.75}$, 10^{-6}, $10^{-6.25}$, $10^{-6.5}$, $10^{-6.75}$, 10^{-7}, $10^{-7.25}$, $10^{-7.5}$, $10^{-7.75}$, 10^{-8}, $10^{-8.5}$ and $10^{-9}\,M_\odot\,yr^{-1}$. This range of accretion spans that necessary to produce stars of between 0.1 and 3 $M_\odot$ within 10^6 yr. The lower rates are similar to those observed in classical T Tauri stars (e.g. Gullbring et al. 1998), while the higher rates correspond to a time average when episodic FU Ori-type events are responsible for the bulk of the mass accretion. These outbursts, with accretion rates of about $10^{-4}\,M_\odot\,yr^{-1}$ lasting about 100 yr and probably recurring every 1000 yr (Hartmann 1991; Kenyon 1999), are necessary to reconcile the very slow accretion, observed in classical T Tauri stars (Gullbring et al. 1998) and in the younger Class I objects (Muzerolle, Hartmann & Calvet 1998), with the higher envelope infall rate (Kenyon et al. 1990). FU Ori events have been successfully modelled as outbursts of high disc-accretion (Hartmann 1991; Bell et al. 1995; Kenyon 1999). The time-scales on which the accretion rate changes are small as far as the stellar evolution of the underlying pre-main-sequence star is concerned, much shorter than its Kelvin–Helmholtz time-scale, and so are not likely to alter the progress of stellar evolution. On the other hand, the thermal time-scale of the outer layers is much shorter, and so a fluctuating accretion rate does have an effect that we should investigate, but one which we cannot follow with our existing machinery, nor one that is likely to alter the luminosity and radius of the star as a whole.

These tracks are plotted in Fig. 2 as thin lines where, for clarity, we terminate them at a mass of 2 $M_\odot$. The ZAMS and zero-age deuterium-burning sequence are added to this figure as dots logarithmically placed in mass. The evolution of a pre-main-sequence star is governed by three competing processes and their associated time-scales. These are gravothermal contraction, accretion and nuclear burning. In the early stages, when the

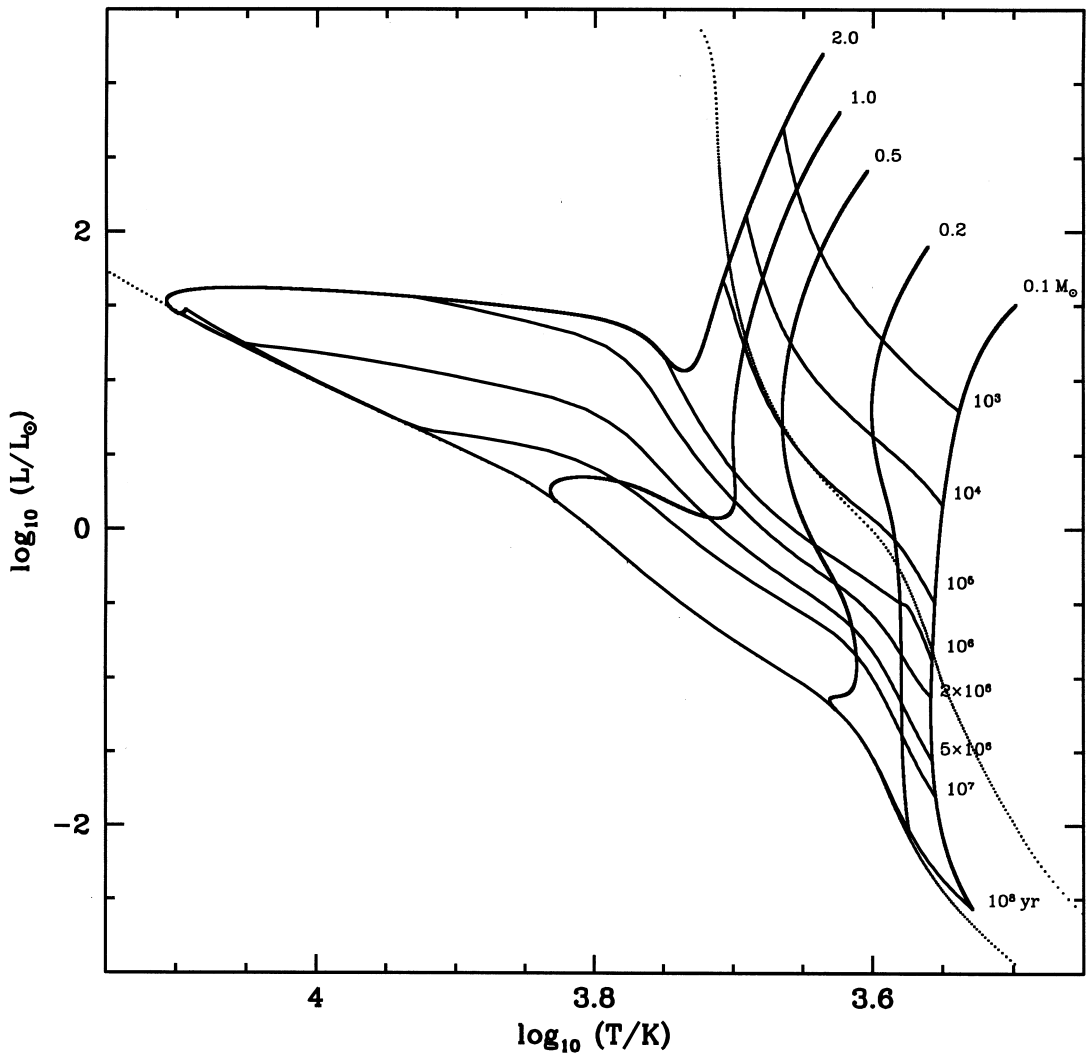

Figure 9. A Hertzsprung–Russell diagram showing constant-mass pre-main-sequence tracks of low metallicity ($Z = 0.001$) stars in the range 0.1 to 2.0 $M_\odot$. Isochrones of ages ranging from 10^3 to 10^8 yr are drawn across the tracks. The models were begun at radii large enough that these isochrones are not affected by small displacements of this starting point. The zero-age main and deuterium-burning sequences appear as dots logarithmically spaced in mass.

Downloaded from https://academic.oup.com/mnras/article/310/2/360/1047159 by guest on 16 May 2021

thermal time-scale τ_{KH} is much shorter than the accretion time-scale $\tau_{\dot{M}}$, the star will evolve down a Hayashi track. If $\tau_{\dot{M}} \ll \tau_{KH}$, it will tend to evolve across to increasing effective temperature to reach a Hayashi track of correspondingly larger mass. Nuclear burning interrupts the contraction once the central temperature is sufficient to ignite a particular reaction and for as long as there is sufficient fuel that the nuclear-burning time-scale $\tau_N > \tau_{KH}$. This first occurs when deuterium ignites, and each track is seen to evolve up the deuterium-burning sequence by an amount that depends on how much mass can be accreted before the deuterium is exhausted. Because these stars are all fully convective, all the deuterium in the star is available for burning, as is any additional deuterium that is accreted at the surface. Subsequently, the tracks are again determined by the competition between $\tau_{\dot{M}}$ and τ_{KH}, but while $\tau_{\dot{M}}$ is only increasing linearly, τ_{KH} is growing almost exponentially with time so that accretion eventually dominates, driving the stars to higher temperature along tracks parallel to the main sequence. At the lowest accretion rates stars descend Hayashi tracks to the ZAMS, and then evolve along it because $\tau_{\dot{M}} \ll \tau_N$. Above $0.3\,M_\odot$, stars develop a radiative core on and just above the main sequence. This causes a contracting pre-main-sequence star to leave its Hayashi track and move to higher temperature before reaching the ZAMS. At the highest accretion rates $\tau_{\dot{M}} \ll \tau_{KH}$ and the stars remain above the main sequence until $M > 2\,M_\odot$. Each of these features is qualitatively described by Hartmann, Cassen & Kenyon (1997), and a direct comparison with their work can be found in Kenyon et al. (1998).

Isochrones, or loci of equal age measured from the zero-age point at $M = M_0$ and $R = R_0$, are drawn as thick lines across the tracks at ages of 10^4, 10^5, 10^6, 2×10^6, 5×10^6, 10^7 and 10^8 yr. The 10^4-yr isochrone lies so close to the initial point, and is consequently so prone to small changes in M_0 or R_0 that it is futile to claim measurements of age below 10^5 yr even if the initial conditions and accretion rate can be estimated. The 10^8-yr isochrone closely follows the ZAMS. Loci where the masses are 0.2, 0.5, 0.8, 1.0 and $2.0\,M_\odot$ are interpolated with thick lines. The actual pre-main-sequence track of a $0.1\text{-}M_\odot$ star is drawn as a thick line to complete the figure.

In Fig. 3 we overlay both the isochrones and the equal-mass loci on the pre-main-sequence tracks and isochrones of Fig. 1 for comparison. During the Hayashi contraction the accreting equal-mass loci follow very closely the tracks of non-accreting

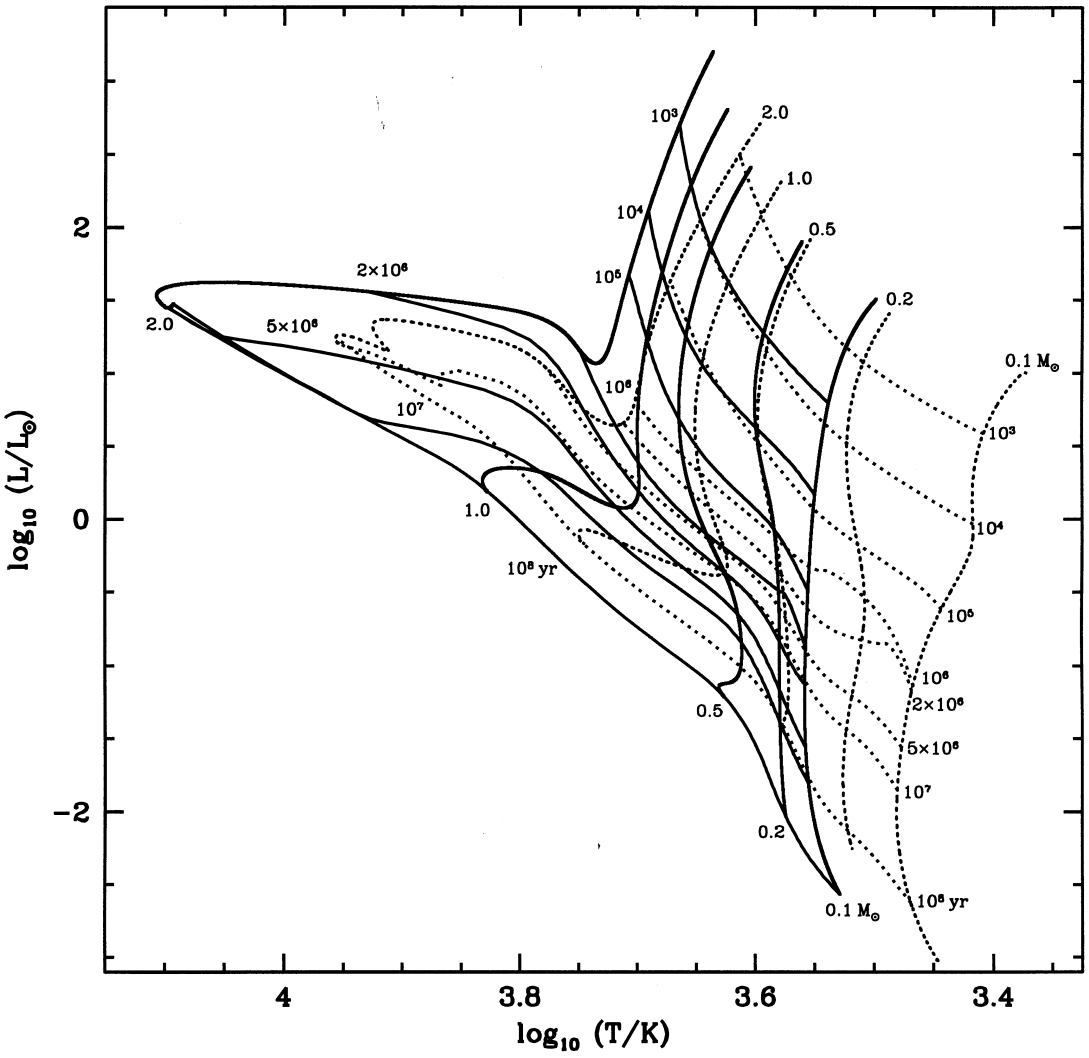

Figure 10. The pre-main-sequence tracks and isochrones for $Z = 0.001$ from Fig. 9 – solid lines – overlaid with those for solar metallicity from Fig. 1 – dotted lines.

Downloaded from https://academic.oup.com/mnras/article/310/2/360/1047159 by guest on 16 May 2021

pre-main-sequence stars, so that determination of a pre-main-sequence star's precise position in the HR diagram gives an equally precise estimate of its mass, irrespective of age and accretion rate. However, once the radiative core forms, an error in the mass determination is introduced. By comparing the change in the slope of the equal-mass loci with the non-accreting tracks we see that accretion delays the effects of the establishment of the radiative core. We note that, up to the point at which the radiative core forms, the fully convective structure has meant that stars evolve essentially homologously. For this reason the approximations used by Hartmann et al. (1997) have remained valid, and we expect their tracks to be a good representation. Once this homology is lost, their equation (6) is no longer valid, nor is their assumption that luminosity is a unique function of mass and radius. The tracks would begin to deviate radically, and it becomes much more important to follow the full evolution as we do here.

Below $0.2\,M_\odot$ and ages greater than 10^6 yr the isochrones are quite similar too, but they deviate drastically for larger masses, with the accreting stars appearing significantly older than they are by factors of two or more according to the non-accreting pre-main-sequence isochrones. This is because, for a given Kelvin–Helmholtz time-scale, a lower mass Hayashi-track star is smaller in radius so that as mass is added and the star moves to higher temperature it always remains smaller and appears older than a star that originally formed with its current mass. As an example, a pre-main-sequence star accreting at $10^{-6.75}\,M_\odot\,yr^{-1}$ would appear to be over 10^7 yr old at $1\,M_\odot$ when it is only 5×10^6 yr old, while one accreting at $10^{-6}\,M_\odot\,yr^{-1}$ at $1\,M_\odot$ would appear to be 5×10^6 yr old when it is only 2×10^6 yr old. Then, because of the delayed appearance of a radiative core, more massive stars begin to appear younger again. For instance, our star accreting at $10^{-7}\,M_\odot\,yr^{-1}$ would appear to remain at 10^7 yr from about 1.3 to $1.74\,M_\odot$, during which time it ages from 1.3 to 1.65×10^7 yr. At ages of less than 10^6 yr the position in the HR diagram depends far more on the starting point than on whether or not the star is accreting, but generally the age will be overestimated by up to the estimate itself.

6 CHANGING R_0 AND M_0

To illustrate the sensitivity of the evolutionary tracks, and the

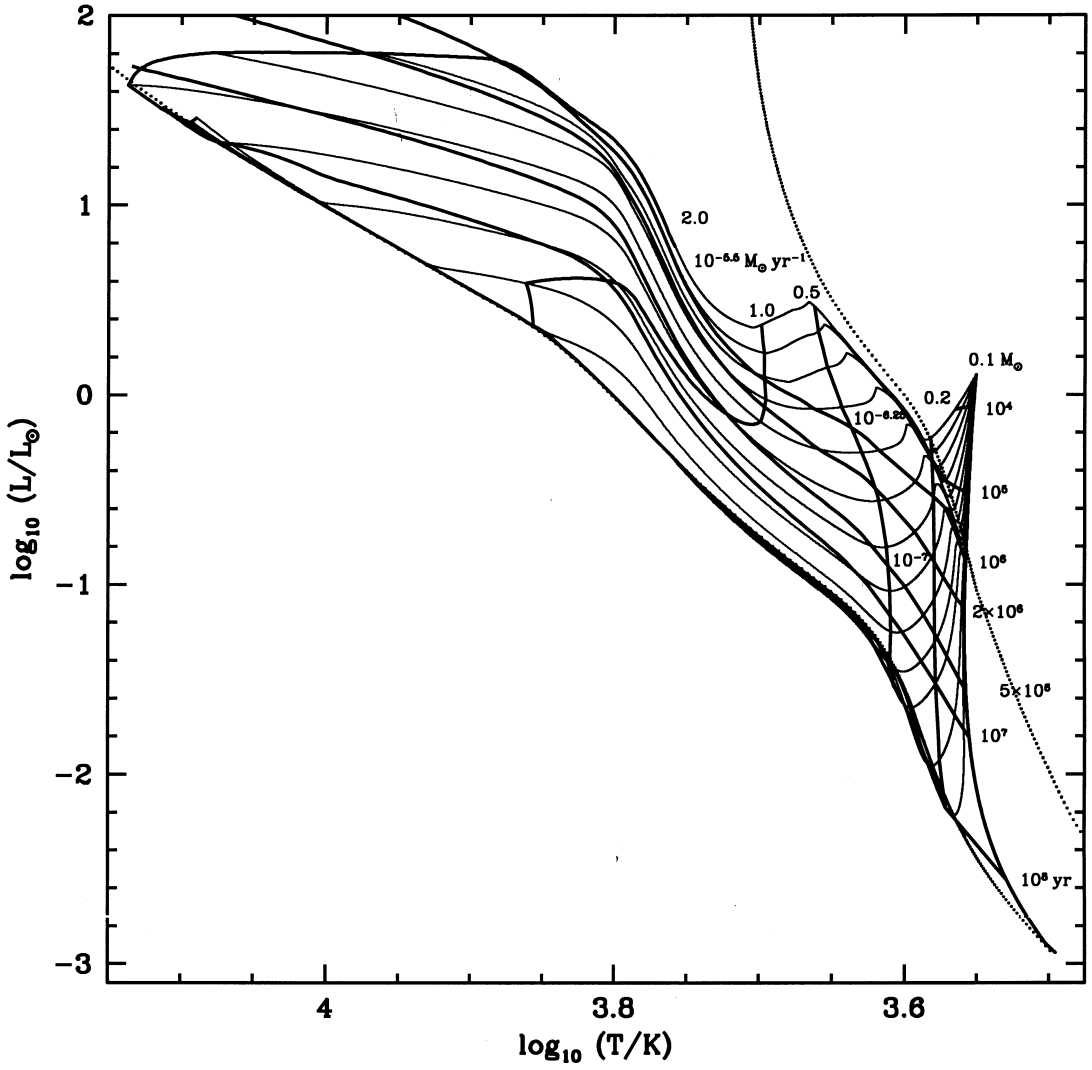

Figure 11. A Hertzsprung–Russell diagram showing, as thin lines, tracks followed by pre-main-sequence stars of initial mass $0.1\,M_\odot$, radius $3\,R_\odot$ and metallicity $Z = 0.001$ evolved with constant accretion rates ranging from 10^{-9} to $10^{-5.5}\,M_\odot\,yr^{-1}$. Thick lines are isochrones of 10^4 to 10^7 yr or join points of equal mass from 0.1 to $2.0\,M_\odot$. The zero-age main and deuterium-burning sequences appear as dots logarithmically spaced in mass.

Downloaded from https://academic.oup.com/mnras/article/310/2/360/1047159 by guest on 16 May 2021

corresponding mass and age determinations, to our choice of initial model, we consider two alternative starting points. First, keeping $M_0 = 0.1\,M_\odot$, we reduce R_0 until the initial protostellar core is just beginning to ignite deuterium. This occurs at about $R_0 = 1.1\,R_\odot$. Second, we reduce M_0 to $0.05\,M_\odot$ and change R_0 to $2.4\,R_\odot$ so as to keep the same mean density. The evolutionary tracks followed by pre-main-sequence stars accreting at the same accretion rates, in the range 10^{-9} to $10^{-5.5}\,M_\odot\,yr^{-1}$, together with isochrones and equal-mass loci are plotted in Figs 4 and 6 respectively. A non-accreting pre-main-sequence track for $0.05\,M_\odot$ in Fig. 6 is seen to run asymptotically down the main sequence. Because its mass is below the hydrogen-burning limit of about $0.08\,M_\odot$, this downward progress to lower luminosities and temperatures will not be halted, and the star will end up as a degenerate brown dwarf.

The isochrones and equal-mass loci are overlaid with those corresponding to our standard tracks in Figs 5 and 7. In neither case are the equal-mass loci significantly affected. Thus the deviation in these loci from non-accreting pre-main-sequence tracks can be solely attributed to the accretion. On the other hand, it is inevitable that the isochrones are affected, but in both cases the difference is small compared with the overall effect of accretion. In the case of reduced R_0 the difference is a constant offset of 10^6 yr. This is just the time taken by a 0.1-$M_\odot$ star to contract from 3 to $1.1\,R_\odot$. Thus ages of about 5×10^6 yr would be accurately estimated to within 20 per cent, and those of about 10^7 yr to within 10 per cent, etc. This error represents the extreme if we can be sure that all stars are born before igniting deuterium. If R_0 were increased beyond $3\,R_\odot$, the initial thermal time-scale would be so short that the time taken to contract to the point of deuterium ignition would not be noticeably different.

From Fig. 7 we can see that the deviations from our standard isochrones are even smaller when $M_0 = 0.05\,M_\odot$. In this case, what is important is the time taken to accrete the additional $0.05\,M_\odot$, and so the most slowly accreting tracks are most affected. Thus the $10^{-9}\,M_\odot\,yr^{-1}$ track reaches $0.1\,M_\odot$ after 5×10^7 yr, leading to a relatively large absolute difference in the 10^8-yr isochrone at $0.1\,M_\odot$. However, as this difference is always relative to the accretion rate, it rapidly becomes insignificant as we go up in mass.

In both these cases it is important to note that the actual tracks followed for a given accretion rate become very similar to our

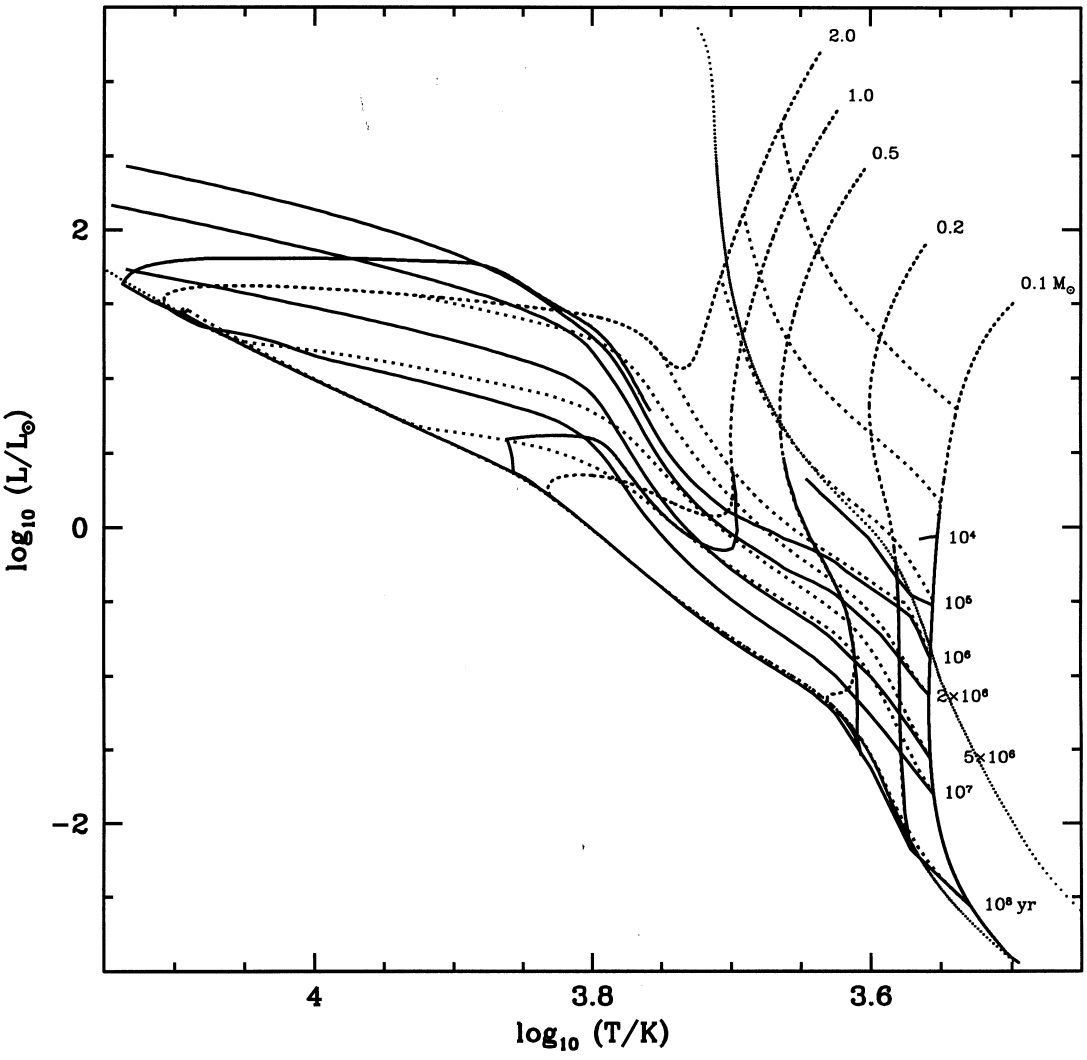

Figure 12. The isochrones and equal-mass loci from Fig. 11 – solid lines – overlaid with the pre-main-sequence tracks and isochrones of Fig. 9 – dotted lines. The zero-age main and deuterium-burning sequences appear as dots logarithmically spaced in mass.

Downloaded from https://academic.oup.com/mnras/article/310/2/360/1047159 by guest on 16 May 2021

standard ones, with the relative time between two points on a track being the same. It is just the time taken to reach an equivalent point that alters the isochrones. We deduce that accretion rate has a much more significant effect on the position in the HR diagram than do the initial conditions.

7 VARIABLE ACCRETION RATES

The models we have presented so far have accreted at a constant rate throughout their pre-main-sequence life. This is unlikely to be the case in reality. Even so, we might hope that a star of a given mass and accretion rate might be found at the intersection of the appropriate accreting track and equal-mass locus of Fig. 2 irrespective of its accretion history. However, we find that this is not the case, because a pre-main-sequence star remembers its past. We illustrate the effect of variable accretion rates by considering three paths, beginning at the same point, that converge to an accretion rate of $10^{-7}\,M_\odot\,yr^{-1}$ when the star's mass reaches $0.5\,M_\odot$ and continue to accrete at that rate, constant thereafter. These tracks are plotted in Fig. 8. The first has the standard constant accretion rate of $10^{-7}\,M_\odot\,yr^{-1}$. The second accretes at a rate that decreases linearly from $10^{-6}\,M_\odot\,yr^{-1}$ at $t = 0$ to $10^{-7}\,M_\odot\,yr^{-1}$ at $0.5\,M_\odot$, while the third has an accretion rate that increases linearly from nothing to $10^{-7}\,M_\odot\,yr^{-1}$. At $0.5\,M_\odot$ we find that the stars are well separated in luminosity. This is to be expected, because a star will take a Kelvin–Helmholtz time-scale to adjust its structure to a new accretion rate. As discussed in Section 5, it is this same time-scale that is balanced with the accretion time-scale that is directly responsible for the deviation of the tracks. This time-scale balance will be maintained until nuclear burning becomes important, in this case on the ZAMS. Consequently, the stars are never given enough time to relax thermally, and their early accretion history can be remembered throughout their pre-main-sequence evolution.

At $1\,M_\odot$ the mass can still be estimated accurately by comparison with the standard accreting tracks of Fig. 2, but note

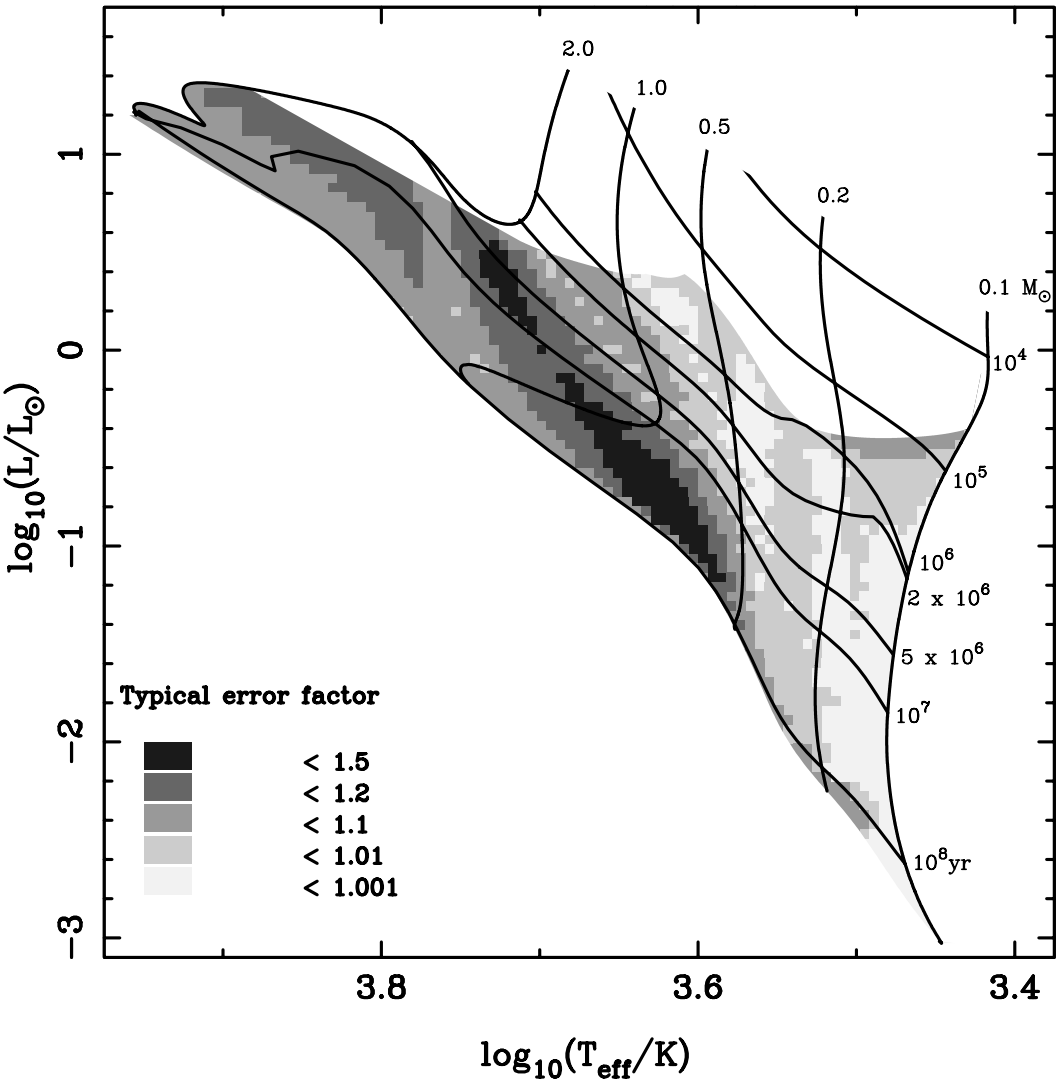

Figure 13. The distribution of the factor by which mass at a given point in the HR diagram differs between our standard accreting tracks and non-accreting tracks. Over most of the diagram the difference is small, being nowhere more than 50 per cent. At temperatures less than about $10^{3.76}$ K the accreting mass is larger, while at higher temperatures the accreting mass is smaller. Some non-accreting tracks and isochrones are overlayed, and the shaded region is that for which we have both accreting and non-accreting tracks available. Twice as many accreting tracks as plotted in Fig. 2 were required to achieve the resolution of this figure.

Downloaded from https://academic.oup.com/mnras/article/310/2/360/1047159 by guest on 16 May 2021

that this differs from the mass that would be estimated if we were to compare with non-accreting tracks. At $0.5\,M_\odot$ age estimates from non-accreting tracks would be between 30 and 60 per cent too old, and at $1\,M_\odot$ between 2 and 3 times too old for each of these stars. This reflects the general nature and magnitude of the difference between non-accreting and our standard accreting pre-main-sequence stars, comparison with which would give a better estimate in each of these particular cases (within 10 per cent at $0.5\,M_\odot$ and 20 per cent at $1\,M_\odot$).

We emphasize again that we cannot estimate the current accretion rate from the position in the HR diagram, but if we know this current rate, then placement in an HR diagram does give us information about the accretion history. This behaviour is in accord with equation (6) of Hartmann et al. (1997), with $\alpha = 0$. As long as $\dot{M}/M$ dominates $\dot{R}/R$, this equation predicts R as a function of M and $\dot{M}$ only. Our track with decreasing $\dot{M}$ always has $\dot{R}/R$ somewhat greater than $\dot{M}/M$, because it has reached $M = 0.5\,M_\odot$ with the two terms in balance at higher accretion rates.

8 CHANGING METALLICITY

Finally, we consider the effect of different metallicities. In general, reducing the metallicity moves the ZAMS to hotter effective temperatures and slightly higher luminosities (see, e.g., Tout et al. 1996). This is due to decreased opacity when there are fewer metal atoms providing free electrons. This shift is reflected throughout the pre-main-sequence evolution. Fig. 9 shows the same tracks and isochrones as Fig. 1 but for a metallicity of $Z = 0.001$. These models have an initial helium abundance of $Y = 0.242$ and a hydrogen abundance of $X = 0.757$ to account for the less-processed interstellar medium from which such stars must be forming. In practice, we should correspondingly increase the deuterium abundance too but, because this is very uncertain anyway, we leave it at $X_D = 3.5 \times 10^{-5}$ so as not to convolute the differences between the two metallicities. Apart from the shift, the tracks are qualitatively similar except for the disappearance of the second hook just above the ZAMS in the more massive star tracks.

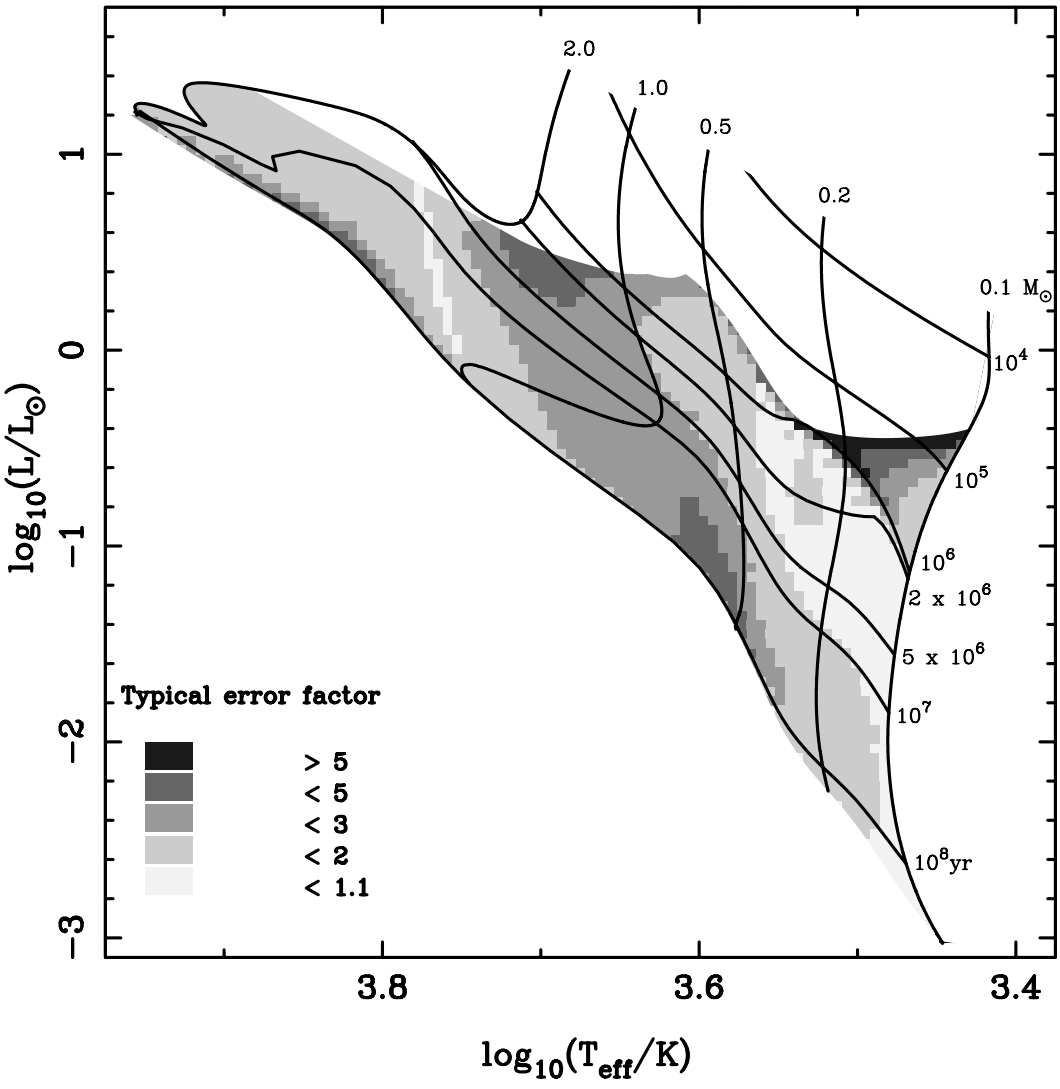

Figure 14. The distribution of the factor by which age at a given point in the HR diagram differs between our standard accreting tracks and non-accreting tracks. For temperatures less than about $10^{3.76}$ K the accreting stars are younger (i.e., they appear older than they are when their age is estimated by comparison with non-accreting tracks), while at higher temperatures they are older. Some non-accreting tracks and isochrones are overlayed, and the shaded region is that for which we have both accreting and non-accreting tracks available. Twice as many accreting tracks as plotted in Fig. 2 were required to achieve the resolution of this figure.

Downloaded from https://academic.oup.com/mnras/article/310/2/360/1047159 by guest on 16 May 2021

At $Z = 0.02$ this is due to the CNO catalytic isotopes moving towards equilibrium in the stellar cores before hydrogen burning begins in earnest.

Fig. 10 overlays these tracks and isochrones with those for $Z = 0.02$. We can see directly that an error of a factor of 2 or more would be made in the mass estimate, and a factor of 10 or so in the age if a pre-main-sequence star of metallicity $Z = 0.001$ were compared with models made for $Z = 0.02$. Clearly, if stars are indeed still forming at such low metallicities, it is very important to be sure of the precise value before making any comparisons. For a rough estimate of how the tracks move with metallicity we interpolate these two sets of tracks together with a similar set for $Z = 0.01$. We find the difference in mass

$$\delta M = M(Z = 0.02) - M(Z) \tag{1}$$

between tracks of metallicity Z and those of solar metallicity that pass through a given point $(L,T_{\rm eff})$ in the HR diagram to be

$$\delta M \approx 0.164\left(\log_{10}\frac{Z}{0.02}\right)^{-0.7}\left(\frac{L}{\mathrm{L}_\odot}\right)^{0.25}\left(\frac{T_{\rm eff}}{10^{3.6}\,\mathrm{K}}\right)^{6} \tag{2}$$

to within 20 per cent before the evolution turns away from the Hayashi tracks.

Fig. 11 shows the accretion tracks starting from the standard initial conditions of $M_0 = 0.1\,\mathrm{M}_\odot$ and $R_0 = 3\,\mathrm{R}_\odot$, together with the associated isochrones and equal-mass loci for $Z = 0.001$. Fig. 12 overlays these with the non-accreting tracks and corresponding isochrones. Similar comments can be made concerning the mass and age determinations as for $Z = 0.02$ from Fig. 3. Note, however, that at this low metallicity all the stars have developed a radiative core before reaching $2\,\mathrm{M}_\odot$.

9 CONCLUSIONS

If the metallicity of a star-forming region is known, then the masses on the Hayashi tracks can be fairly accurately determined.

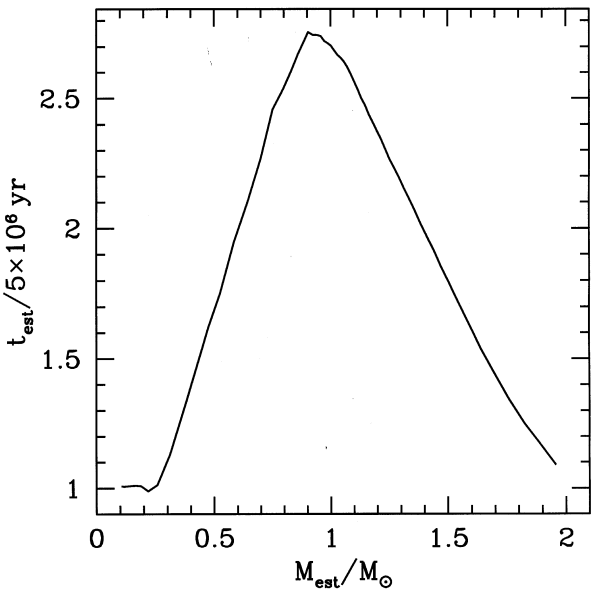

Figure 15. The estimated age and mass for each point along the 5×10^6 yr fitted to our standard accreting tracks (Fig. 2) when the luminosity and effective temperature are compared with the non-accreting tracks of Fig. 1.

As noted by Siess et al. (1997), accretion delays the formation of a radiative core, which consequently begins further down the Hayashi track at a given mass. However, the locus of equal-mass points will subsequently move to higher luminosities than a non-accreting star of the same mass. Thus the mass determined by comparison with the Henyey portion of any track can be either an underestimate or an overestimate. Fig. 13 shows the relative error that might be made in estimating the mass over the region of interest in the HR diagram. In the Hayashi region accretion generally leads to an overestimate of the age in a comparison with non-accreting tracks, while it can lead to an underestimate during the Henyey phase. At any time these errors in age could be a factor of 2 or more. Fig. 14 illustrates the error distribution for age estimates. In addition, not knowing the zero-age mass and radius of the star can lead to an absolute offset in age of up to about 10^6 yr, so that any age estimate of less than about 2×10^6 yr cannot be trusted. Ages larger than this can be significantly in error if accretion is taking place at an unknown rate but, once accretion has ceased, the age can be expected to correspond to non-accreting isochrones within a Kelvin–Helmholtz time-scale. Thus the absolute error would be about equal to the age at which accretion became insignificant. In all other cases great care must be taken when estimating ages.

Apart from the initial comparatively small offsets, even if the initial conditions of a set of stars are known to be the same, relative ages are equally affected by accretion history. As a particular example, we may wish to decide whether two components of a pre-main-sequence binary star are coeval. If, as pre-main-sequence stars often do, one or both lies in the temperature range between $10^{3.55}$ and $10^{3.75}$ K where the error in age is likely to be more than a factor of 2, we can expect a significant difference in estimated age even in a coeval system. This binary example can be extended to star clusters. Accretion can lead to an apparent mass-dependent age-spread in otherwise coeval systems when non-accreting pre-main-sequence tracks are used to estimate ages. At any time, if all the stars in a cluster are coeval and began with the same initial core mass, the low-mass stars must have accreted less and hence have lower disc-accretion rates than those of higher mass which must have accreted more material. Thus accretion does not greatly affect the age determination of low-mass stars while higher mass stars are more affected. Comparison with non-accreting tracks makes these appear older while on Hayashi tracks and younger on the Henyey tracks (see Fig. 14). Thus, intermediate-mass pre-main-sequence stars can look older than their low-mass counterparts (by up to a factor of 5) while yet higher mass stars can appear younger again. Fig. 15 illustrates this point by plotting the estimated age against the estimated mass for all points along the 5×10^6 yr isochrone fitted to our standard accreting tracks. Although this is a particular case for a particular set of models, this qualitative behaviour would be true of any coeval sample that is still undergoing accretion. Indeed, mass-dependent ages have been recorded in several young stellar clusters where the lowest mass stars appear youngest, with increasing ages for the intermediate-mass stars and lower ages again for the higher mass stars (Carpenter et. al. 1997; Hillenbrand 1997). These mass-dependent ages may reflect ongoing disc-accretion rather than a dispersion in formation time, and age determinations in these clusters should be re-evaluated in the light of this work.

If the metallicity is not known, the situation becomes even worse. For instance, as mentioned in the introduction, the metallicity of some extragalactic star-forming regions, and

Downloaded from https://academic.oup.com/mnras/article/310/2/360/1047159 by guest on 16 May 2021

possibly even Orion, may be as low as $Z = 0.001$. This would lead to an overestimate in mass by a factor of 2 or more, and an overestimate in age by about a factor of 10, if a comparison were inadvertently made with solar-metallicity tracks.

ACKNOWLEDGMENTS

CAT and IAB are very grateful to PPARC for advanced fellowships. CAT also thanks NATO, the SERC and the University of California in Santa Cruz for a fellowship from 1990 to 1991 when much of the foundation for this work was laid, and the Space Telescope Science Institute for an eight-month position during which it was continued. Many thanks go to Jim Pringle for mild but chronic goading, and for many ideas and suggestions along the way.

REFERENCES

Alexander D. R., Ferguson J. W., 1994, ApJ, 437, 879
Anders E., Grevesse N., 1989, Geochim. Cosmochim. Acta, 53, 197
Baraffe I., Chabrier G., Allard F., Hauschildt P. H., 1995, ApJ, 446, L35
Bell K. R., Lin D. N. C., Hartmann L. W., Kenyon S. J., 1995, ApJ, 444, 376
Boss A. P., 1987, ApJ, 316, 721
Carpenter J. M., Meyer M. R., Dougados C., Strom S. E., Hillenbrand L. A., 1997, AJ, 114, 198
Cohen M., Kuhi L. V., 1979, ApJS, 41, 743
D'Antona F., Mazzitelli I., 1994, ApJS, 90, 467
Eggleton P. P., 1971, MNRAS, 151, 351
Eggleton P. P., 1972, MNRAS, 156, 361
Eggleton P. P., 1973, MNRAS, 163, 279
Gullbring E., Hartmann L., Briceno C., Calvet N., 1998, ApJ, 492, 323
Hartmann L., 1991 in Lada C., Kylafis N., eds, The Physics of Star Formation and Early Stellar Evolution. Kluwer, Dordrecht, p. 623
Hartmann L., Cassen P., Kenyon S. J., 1997, ApJ, 475, 770
Hayashi C., 1961, PASJ, 13, 450
Henyey L. G., Lelvier R., Levee R. D., 1955, PASP, 67, 154
Hillenbrand L. A., 1997, AJ, 113, 1733
Iglesias C. A., Rogers F. J., Wilson B. G., 1992, ApJ, 397, 717(OPAL)
Kenyon S. J., 1999, in Lada C., Kylafis N., eds, The Physics of Star Formation and Early Stellar Evolution II. Kluwer, Dordrecht, in press
Kenyon S. J., Brown D. I., Tout C. A., Berlind P., 1998, AJ, 115, 2491
Kenyon S. J., Hartmann L. W., Strom K. M., Strom S. E., 1990, AJ, 99, 869
Kroupa P., Tout C. A., 1997, MNRAS, 287, 402
Larson R. B., 1969, MNRAS, 145, 271
Larson R. B., 1984, MNRAS, 206, 197
Lin D. N. C., Pringle J. E., 1990, ApJ, 358, 515
Low C., Lynden-Bell D., 1976, MNRAS, 176, 367
Mercer-Smith J. A., Cameron A. G. W., Epstein R. I., 1984, ApJ, 279, 363
Muzerolle J., Hartmann L., Calvet N., 1998, AJ, 116, 2965
Palla F., Stahler S. W., 1993, ApJ, 418, 414
Pols O. R., Tout C. A., Eggleton P. P., Han Z., 1995, MNRAS, 274, 964
Rees M. J., 1976, MNRAS, 176, 483
Rubin R. H. et al., 1997, ApJ, 474, L131
Siess L., Forestini M., 1996, A&A, 308, 472
Siess L., Forestini M., Bertout C., 1997, A&A, 326, 1001
Stahler S. W., 1983, ApJ, 274, 822
Stahler S. W., 1988, ApJ, 332, 804
Stahler S. W., Shu F. H., Taam R. E., 1980a, ApJ, 241, 637
Stahler S. W., Shu F. H., Taam R. E., 1980b, ApJ, 242, 226
Stahler S. W., Shu F. H., Taam R. E., 1981, ApJ, 248, 727
Tout C. A., Pols O. R., Eggleton P. P., Han Z., 1996, MNRAS, 281, 257
Tout C. A., Aarseth S. J., Pols O. R., Eggleton P. P., 1997, MNRAS, 291, 732
Warner B., 1995, Cataclysmic Variable Stars. Cambridge Univ. Press, Cambridge
Winkler K.-H.A., Newman M. J., 1980, ApJ, 238, 311
Woolley R.v.d.R., Stibbs D. W. N., 1953, The Outer Layers of a Star. Clarendon Press, Oxford

This paper has been typeset from a TEX/LATEX file prepared by the author.

Downloaded from https://academic.oup.com/mnras/article/310/2/360/1047159 by guest on 16 May 2021